Available online at www.sciencedirect.com
ScienceDirect
Applied Geochemistry 22 (2007) 1329–1343
Applied Geochemistry
www.elsevier.com/locate/apgeochem

Diel variations in stream chemistry and isotopic composition of dissolved inorganic carbon, upper Clark Fork River, Montana, USA

Stephen R. Parker [a,*], Christopher H. Gammons [b], Simon R. Poulson [c], Michael D. DeGrandpre [d]

[a] *Department of Chemistry and Geochemistry, Montana Tech of The University of Montana, 1300 West Park Street, Butte, MT 59701, USA*
[b] *Department of Geological Engineering, Montana Tech of The University of Montana, Butte, MT 59701, USA*
[c] *Department of Geological Sciences, University of Nevada-Reno, Reno, NV 89557, USA*
[d] *Department of Chemistry, The University of Montana, Missoula, MT 59812, USA*

Received 21 December 2005; accepted 16 February 2007
Editorial handling by B. Kimball
Available online 20 March 2007

Abstract

Many rivers undergo diel (24-h) concentration fluctuations of pH, dissolved gases, trace metals, nutrients, and other chemical species. A study conducted in 1994 documented such behavior in the upper Clark Fork River, Montana, a stream whose headwaters have been severely impacted by historic metal mining, milling, and smelting. The purpose of the present investigation was to expand on these earlier findings by conducting simultaneous diel samplings at two sites on the upper Clark Fork River separated by 2.5 h of stream travel time. By monitoring two stations, it was possible to more closely examine the processes that control temporal and spatial gradients in stream chemistry. Another objective was to examine diel changes in the $\delta^{13}C$ composition of dissolved inorganic C (DIC) and their relationship to biological activity in the stream. The most important findings of this study include: (1) concentrations of dissolved and particulate heavy metals increased during the night and decreased during the day, in agreement with previous work; (2) these changes were positively correlated to diel changes in pH, dissolved O_2, and water temperature; (3) dissolved NO_3 concentrations increased during the night at the lower site, but showed the opposite behavior at the upper site; and (4) diel changes in $\delta^{13}C$-DIC were noted at both sites, although the timing and magnitudes of the cycles differed. Hypotheses to explain the first two observations include: cyclic co-precipitation of divalent metals with carbonate minerals; pH- and temperature-dependent sorption of metal cations onto the streambed and suspended particles; or photosynthetically enhanced oxidation and removal of Fe and Mn oxides at biofilm surfaces during the daytime. The latter model explains the majority of the field observations, including night-time increases in particulate forms of Fe and other elements.

1. Introduction

In the past 16 years, there have been an increasing number of publications focusing on diel (24-h)

* Corresponding author.
E-mail address: sparker@mtech.edu (S.R. Parker).

0883-2927/$ - see front matter
doi:10.1016/j.apgeochem.2007.02.007

fluctuations in the concentrations of metals and other chemical species in rivers and streams. For example, Fuller and Davis (1989) and Nimick et al. (1998) documented daytime increases in dissolved As concentration of up to 40% in alkaline streams and rivers of the northern Rocky Mountains. Much larger diel variations of up to 500% have been documented for cationic metals: including Zn, Mn and Cd (Brick and Moore, 1996; Bourg and Bertin, 1996; Nimick et al., 2003, 2005; Jones et al., 2004); Hg (Nimick et al., 2007); Fe and Cu (McKnight et al., 1988; Gammons et al., 2005a; Parker et al., 2006); and rare earth elements (Gammons et al., 2005b; Wood et al., 2006). Daily cycles of temperature, oxidation–reduction, photosynthesis and respiration force cyclic chemical and physical changes in parameters such as pH, alkalinity, specific conductivity, dissolved O_2, redox speciation, dissolved CO_2, and dissolved and particulate trace and major element concentrations. Riverine transport of metals and metalloids and future impacts from development and climate change can have a significant effect on aquatic and human health. For cases where the concentration of a contaminant of concern varies over a diel time period, the time of day in which a river sample is collected could have a large bearing on whether the water passes or exceeds a regulatory standard. For this reason, sampling programs designed to monitor water quality of rivers and streams should take diel processes into account.

Despite the increasing number of field studies documenting diel changes in trace metal concentrations in streams, there is still considerable uncertainty as to specific chemical or biological mechanisms that control these cycles (e.g. see Nimick et al., 2003, for a recent review). It is generally accepted that diel pH and redox cycles in rivers are largely driven by aquatic plants and microbes (Odum, 1956; Pogue and Anderson, 1994; Nagorski et al., 2003; Jones et al., 2004). During the day when the rate of photosynthesis exceeds that of respiration, CO_2 is consumed, O_2 is produced, and the temperature, pH and oxidation state of the water column and aquatic biofilms all increase. At night, in the absence of photosynthesis, respiration reverses these trends. The changes in environmental variables such as pH and Eh clearly have a major control on diel metal and nutrient cycles. However, in most cases it is not known whether metals are present in the solid phase as adsorbed ions, as discrete mineral phases, or as impurities in more common minerals, such as calcite. In addition, it is typically not known whether the microbial community plays an active or passive role in metal and nutrient sequestration.

The complex natural variability of streams requires that additional techniques be employed to constrain these sources of variability. The C isotope ($^{13:12}C$) composition of dissolved inorganic C ($\delta^{13}C$-DIC) has been used as a tracer for studying biogeochemical processes in rivers and streams (Usdowski et al., 1979; Spiro and Pentecost, 1991; Tobias and Bohlke, 2004; Silva et al., 2004; Parker et al., 2005). The $\delta^{13}C$-DIC of a river is determined by a balance of the effects of photosynthesis, respiration, gas exchange, groundwater contributions and carbonate mineral precipitation or dissolution reactions. Aquatic plants use CO_2 during photosynthesis and there is a C isotope fractionation associated with this process. When the supply of dissolved CO_2 is not limiting, $^{12}CO_2$ is consumed faster than $^{13}CO_2$ (Falkowski and Raven, 1997). Conversely, plant and microbial respiration typically produce CO_2 that has an isotopic signature similar to that of the indigenous vegetation. In temperate regions, C_3 plants are the dominant species; with $\delta^{13}C$ organic C values in the range of $-20‰$ to $-30‰$ (Clark and Fritz, 1997). Thus, biogenically produced CO_2 is normally isotopically light relative to atmospheric CO_2 which in the western USA is typically in the range of $-7‰$ to $-8.5‰$ (NOAA, 2006). Consequently, the $\delta^{13}C$-DIC should increase during the day when photosynthesis is the dominant process and decrease at night in the absence of photosynthesis when respiration is the dominant process.

In an early study on diel cycling in rivers, Brick and Moore (1996) described diel phenomena in the upper Clark Fork River, a mining-impacted stream in SW Montana. One of the objectives of the present study was to test the reproducibility of the diel trends observed by Brick and Moore (1996) by conducting a follow-up investigation of the upper Clark Fork River at the same general location. A more detailed sampling methodology has been employed in which two sites (an upstream and downstream site, separated by several hours of water travel time) were simultaneously monitored. This approach allows for a more detailed refinement of the rates and mechanisms of the observed diel cycles, as well as improved definition of spatial heterogeneity in the timing and magnitude of these cycles. Finally, data are reported on the diel varia-

tion in δ^{13}C-DIC of the Clark Fork River, and mechanisms discussed – both inorganic and biological that likely play a role in the observed diel cycles of C isotope ratios, as well as the concentrations of dissolved metals and nutrients.

1.1. Location

The upper Clark Fork River (CFR) is located in southwestern Montana, USA and is a major tributary of the Columbia River. The study area is located upstream (south) of the town of Deer Lodge (Fig. 1), and in this section the Clark Fork is a small, second order stream with a discharge of roughly 0.6–60 $m^3 s^{-1}$, depending on the time of year. The mining and smelting centers of Butte and Anaconda are situated at the headwaters of the upper Clark Fork River along Silver Bow and Warm Springs Creeks, respectively (Fig. 1). The floodplain and streambed of Silver Bow Creek and the upper Clark Fork River contain highly elevated quantities of metals and metalloids (As, Fe, Cu, Zn, Pb and Cd) deposited by the mining, milling and smelting activities (Moore and Luoma, 1990). Most of the heavy metal load in Silver Bow Creek is removed by a lime treatment facility as the water enters the Warm Springs Ponds (Fig. 1). However, concentrations of dissolved As in water exiting the treatment ponds are elevated (20–50 μg L^{-1}) during summer base-flow periods (Duff, 2001; Grant, 2006).

Two sampling sites were selected for detailed monitoring and sampling. The upstream site was designated AS1 (46 22.64′N, 112 44.26′W) and the downstream site, AS2 (46 23.36′N, 112 44.21′W) (Fig. 1). The AS2 sampling site was approximately 2.4 km upstream from the site used in the 1994 study of Brick and Moore (1996). The AS1 and AS2 sites were separated by about 1.2 km river distance, about 25 m in elevation, and had a mean water transit time of about 2.5 h. The river in the study reach has moderate alkalinity (3200 to 3700 μmol kg^{-1}), moderate biological productivity (AS1: 97 ± 6 mg m^{-2} chlorophyll; V. Watson, personal communication) and a pH range of about 8.0–9.0 during the summer months. Aquatic plants are dominated by *Cladophora* and diatom algae (Watson, 1989). During the mid-summer months, water in the Clark Fork River and its tributary streams is diverted for irrigation. Some of this water returns to the main stem in a chemically modified form as surface or groundwater return flow. This

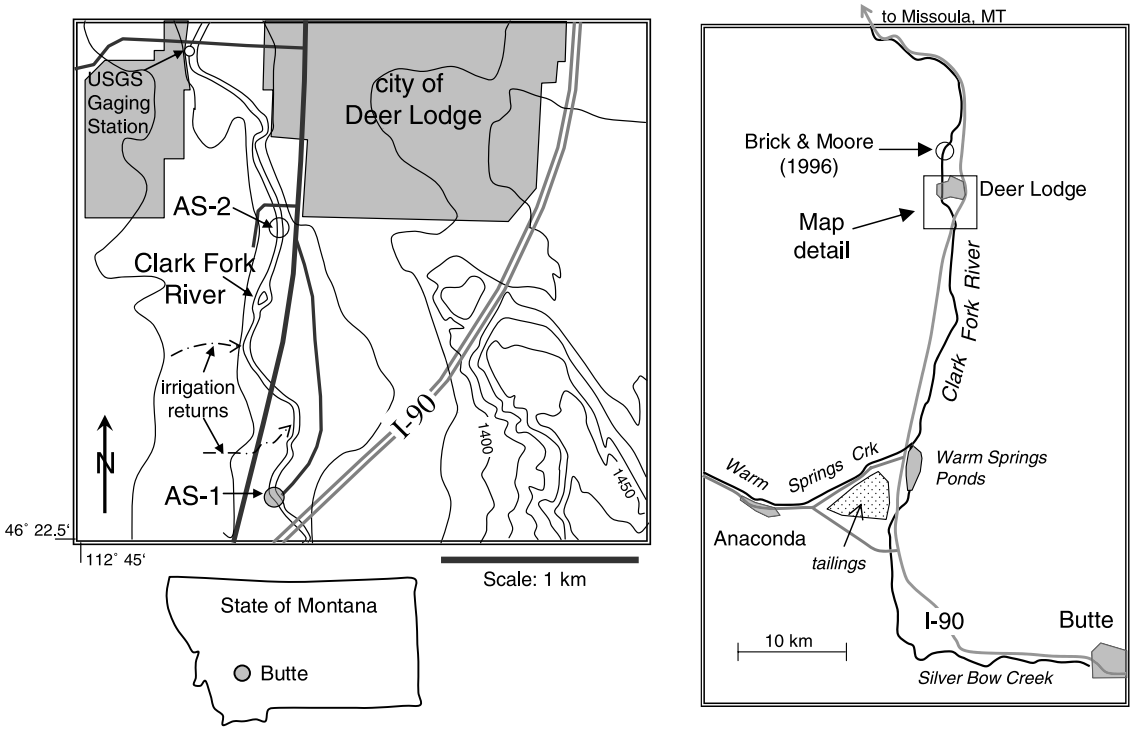

Fig. 1. Map of Clark Fork River study area south of Deer Lodge, MT and sampling sites AS1 and AS2.

greatly complicates the hydrogeology and nutrient balance of the watershed.

2. Methods

The diel sampling event took place from 11:00 h on 31 July to 10:00 h on 01 August 2003. All times are reported as local time (MDT, GMT 06:00). Selected data were collected until 14:00 h on the second day.

Streamflow was continuously monitored at AS1 using the stage-discharge method (Rantz, 1982). The total range in flow during the study period at AS1 was small, with a minimum flow of 0.67 $m^3 s^{-1}$ at 18:00 h on 31 July, and a maximum flow of 0.69 $m^3 s^{-1}$ at 10:00–13:00 h on the following day. Streamflow at AS2 was measured at the beginning and the end of the study period and averaged 0.79 $m^3 s^{-1}$. The 15% increase in flow (roughly 0.1 $m^3 s^{-1}$) between AS1 and AS2 was mostly due to the influx of several irrigation return tributaries and groundwater seeps (Fig. 1). This increase in flow was assumed to be more or less constant during the sampling period. The water transit time between AS1 and AS2 was determined by the addition of a NaCl tracer at the upstream site followed by monitoring SC at the downstream site.

Water samples were collected on the hour at the AS1 (upstream) site and on the half hour at AS2 for the full 24-h period using an automated collection system with 500 mL high density polyethylene (HDPE) bottles. Four bottles were collected each hour at each site. All sample and collection bottles were acid washed (5%, v/v HNO_3) prior to the field work and triple rinsed with deionized water. The samples were transported within 10 min of collection to a field laboratory in Deer Lodge. Raw and filtered water samples were collected for inductively coupled plasma atomic emission spectroscopy (ICP-AES) analysis using 125 mL HDPE bottles. Filtered samples were processed using a peristaltic pump and disposable 142 mm diameter 0.1-μm cellulose-ester filter membranes (see also Gammons et al., 2005a). In this paper, the term "dissolved" refers to any substance that passed through the 0.1-μm filters. A clean filter was used for each sample. Field blanks were collected at the beginning and end of the sampling period by processing deionized water through the same filtration and preservation protocols as for the samples. Several field duplicate samples were also collected. All samples for ICP-AES analysis were acidified in the field to 1% (v/v) with concentrated Optima HNO_3.

The *partial pressure of CO_2* (pCO_2) and *photosynthetically active radiation* (PAR) were measured at both sites using two *in situ* Submersible Autonomous Moored Instruments (SAMI-CO_2) instruments (DeGrandpre et al., 1995, 1999). The SAMI-CO_2 instruments were calibrated prior to deployment, and precision of the wet CO_2 partial pressures is estimated to be ±12 μatm at 1400 μatm (Baehr and DeGrandpre, 2004). A Li-COR Inc., LI-192SA detector was used for the PAR flux values (μE $m^{-2} s^{-1}$) which were based on the manufacturer's calibration of the sensor.

Field parameters, including pH, temperature, dissolved O_2 (DO) and specific conductance (SC), were collected in several different ways. Field pH at both sites was determined colorimetrically using unfiltered water, following the method of French et al. (2002). The accuracy of this method is ±0.01 pH units (French et al., 2002). Field pH, temperature, DO and SC were continuously measured at AS1 using a Hydrolab Datasonde 3. The SC and DO electrodes were calibrated immediately prior to deployment. Post deployment calibration checks showed that the SC was within 0.5% of calibration and DO was within 10% of calibration. Handheld meters were used at both sites as a backup to record hourly changes in pH, SC, DO and water temperature. Because of their higher precision and accuracy, the colorimetric pH measurements were used for the geochemical modeling described later in this paper, and for all graphical presentations.

Total alkalinity of unfiltered water was measured onsite by the open-cell potentiometric titration method (Dickson et al., 2003) and Gran plot analysis (Edmond, 1970). This method is estimated to have a precision within ±10 μequiv. kg^{-1} based on replicate titrations and an accuracy of ±10 μequiv. kg^{-1} based on the titration of four sodium carbonate standards.

Dissolved nitrate and chloride concentrations were determined in the field on filtered samples using a HACH model DR/2010 portable spectrophotometer. Nitrate was determined by the Cd reduction method 8192 with an estimated precision of ±0.04 mg NO_3 (as NO_3) L^{-1} based on replicate measurements, and a PQL of 0.04 mg L^{-1}. Chloride was determined by the mercuric thiocyanate method 8113 with a precision of ±0.3 mg L^{-1} (3%).

Dissolved Fe species were determined colorimetrically in the field using the Ferrozine method (To et al., 1999). However, all of the concentrations were near or below the analytical detection limit (roughly 0.01 mg L $^{-1}$) at all times.

Total suspended solids (TSS) were quantified for raw water samples from AS1. Each hour a 1-L sample was filtered through a pre-weighed (mass reproducible to ±0.001 g) fiberglass filter. All filters were subsequently dried at 50 C for 2 days prior to weighing.

Major and trace element concentrations of acid-preserved filtered and unfiltered samples were determined by inductively coupled plasma atomic emission spectroscopy (ICP-AES) using EPA method 200.15 and a Thermo Jarrell Ash model IRIS ICP. Field and laboratory duplicate samples for the elements reported in this study agreed within 10%. Spike recovery for all elements was within 85–115%. Values obtained by ICP analysis of the field blanks were all below the practical quantifiable limits (PQL) for Al, As, Cu, Fe, S and Zn. The Ca and Mn concentrations of field blanks were above the PQL, but were 0.3% and 2.7%, respectively, of the average measured values of all samples. The ICP-AES data for S and P were used to calculate SO_4 and PO_4 concentrations, assuming that these were the dominant forms of each element in solution. The average measured P concentration was 80% of the laboratory PQL, but was 6 times higher than the value reported for the field blank.

Samples for *carbon isotope analysis* were processed in the field using filtered water and precipitation of aqueous dissolved inorganic C (DIC) as $SrCO_3$, after the method of Usdowski et al. (1979). Stable C isotope analyses of $SrCO_3$ extractions were performed at the University of Nevada-Reno, following the method of Harris et al. (1997). Isotope values are reported in units of parts per thousand (‰) in the usual δ notation versus VPDB. Replicate analyses indicate an analytical uncertainty of ±0.05‰ for δ^{13}C-DIC.

3. Results

3.1. Field parameters

Diel changes in pH, water temperature (C), partial pressure of dissolved CO_2 (pCO_2, μatm), total alkalinity (TA, μmol kg $^{-1}$), specific conductance (SC, μS cm $^{-1}$) and dissolved O_2 (DO, μmol L $^{-1}$) from both sampling sites are shown in Fig. 2. The diel change in pH at both sites was approximately 0.5 pH units, and the 24-h change in stream temperature was 8.0 C at AS1 and 7.7 C at AS2. Alkalinity and SC showed small (less than 5%) changes over the study period. The pCO_2 and DO concentrations varied over a much wider range and were inversely related, which is typical of streams with moderate to high biological productivity. DO increased to levels greater than 150% of local atmospheric saturation during the day, and dropped to levels as low as 65% of saturation at night. The pCO_2 at both sites was higher than the atmospheric value (328 μatm) during the entire experimental period, driving a net flux of CO_2 from the water to the air.

The total suspended solids (TSS, mg kg $^{-1}$) measured at the AS1 site underwent a 3.6-fold increase during the night, with the maximum concentration occurring between 01:00 and 06:00 h (Fig. 3, TSS was not measured at AS2). A similar increase in particulate metal concentrations during the night was noted by Brick and Moore (1996) in their previous study of the upper Clark Fork River. Possible reasons for this phenomenon are discussed below.

3.2. Trace elements

Of the trace metals and metalloids analyzed (Al, As, Cu, Fe, Mn and Zn) Mn and Zn showed the largest diel concentration changes. Concentrations of dissolved Mn and Zn at both sites increased during the night by 100% and 500%, respectively (Fig. 4). The concentration of suspended particles of Mn and Zn (calculated by the difference of filtered and unfiltered concentrations) increased during the night at AS1 (coincident with the increase in TSS), but not at AS2 (Fig. 4). Additionally, significant diel cycles in particulate forms of Fe, Al and Cu were found at both AS1 and AS2 (Fig. 5). Dissolved Al was below detection at both AS1 and AS2 while dissolved Cu and Fe were near detection and showed no diel pattern. Dissolved As was elevated at both sites (14–18 μg L $^{-1}$), but also did not show a clear diel pattern. Overall, the timing and magnitude of the diel metal cycles observed in this study are similar to those previously reported by Brick and Moore (1996).

3.3. Nutrients

The concentration of dissolved NO_3 at AS1 was consistently lower than at AS2, and dropped to

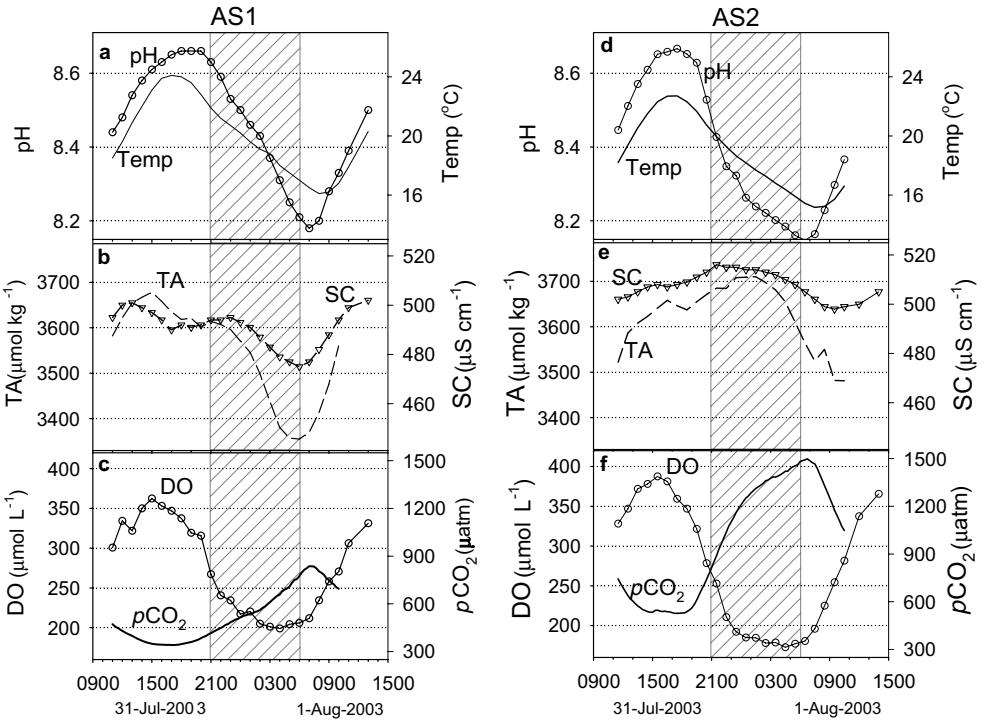

Fig. 2. AS1 site parameters: (a) pH and temperature (°C); (b) total alkalintiy (TA, μmol kg^{-1}) and specific conductivity (SC, μS cm^{-1}); (c) dissolved O_2 (DO, μmol L^{-1}; 79.6–158.0% sat) and pCO_2 (μatm). AS2 site parameters: (d) pH and temperature (°C); (e) total alkalintiy (μmol kg^{-1}) and specific conductivity (μS cm^{-1}); (f) dissolved O_2 (μmol L^{-1}; 66.6–167.0% sat) and pCO_2 (μatm). Shaded area approximates the dark period based on the lack of a PAR flux (Fig. 3).

levels below the detection limit of the field colorimeter during the night (Fig. 6). In contrast, NO_3^- levels at AS2 rose slightly during the night. The latter pattern was also noted by Brick and Moore (1996) in their 1994 study. The differences in NO_3^- concentration between AS1 and AS2 were most likely caused by NO_3^--rich irrigation return flows that entered the river between the two stations, both as surface runoff and as groundwater. Two small tributaries draining irrigated fields below AS1 were sampled on 31 July between 15:00 and 17:00 h, and had NO_3^- concentrations of 1.8 and 1.4 mg NO_3^- L^{-1}. These concentrations were approximately 20 times higher than NO_3^- in the main upstream flow at AS1 (~0.08 mg NO_3^- L^{-1}) during the same time period.

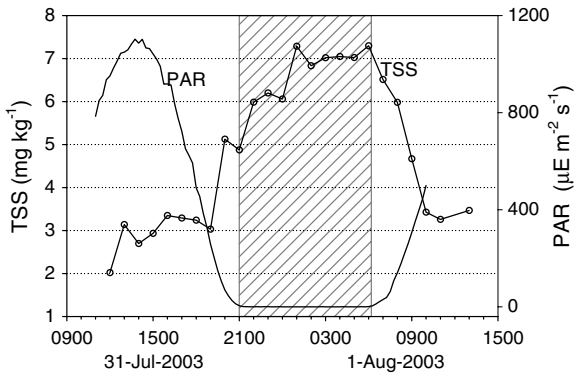

Fig. 3. Total suspended solids (TSS, mg kg^{-1}) and photosynthetically active radiation (PAR, μE m^{-2} s^{-1}) at AS1.

Unlike NO_3^-, the concentration of dissolved PO_4^{3-} PO_4 (based on ICP-AES total dissolved P analyses) did not vary significantly at either site during the period of investigation, and furthermore showed no between site changes (data not shown).

3.4. Carbon isotopes

Diel changes in the isotopic composition of DIC (δ^{13}C-DIC) are summarized in Fig. 7. At both AS1 and AS2, the 24-h changes in δ^{13}C-DIC were small (less than 1.0‰), but were nonetheless considerably greater than the analytical precision (estimated at ±0.05‰). The shape of the δ^{13}C-DIC versus time trend was quite different at the two stations. Whereas both sites showed an increase in δ^{13}C-DIC in the afternoon of the first day, the δ^{13}C

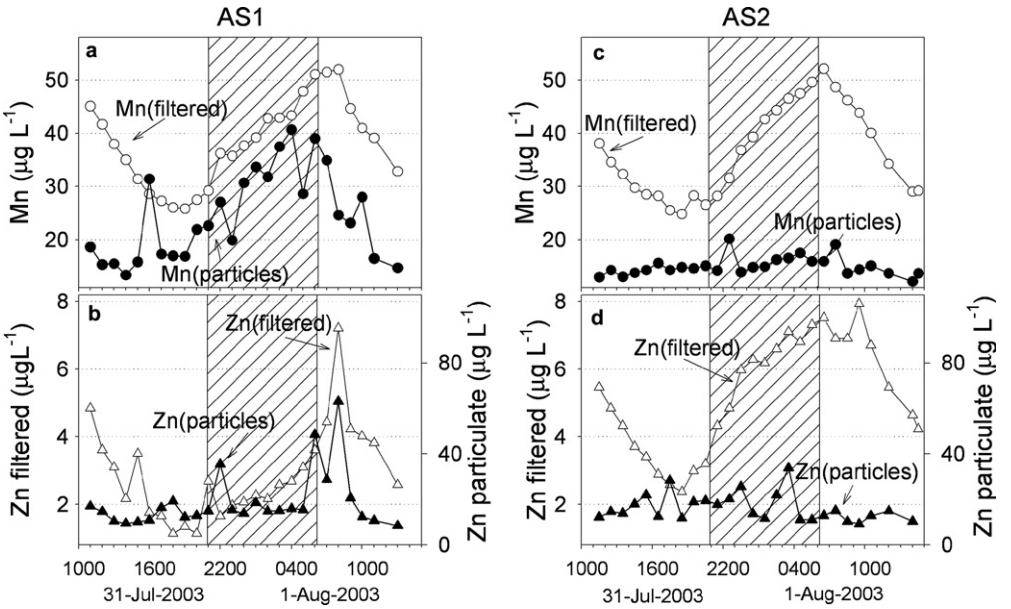

Fig. 4. (a) AS1 concentrations of dissolved and particulate Mn (μg L $^{-1}$); (b) AS1 concentrations of dissolved and particulate Zn (μg L $^{-1}$); (c) AS2 concentrations of dissolved and particulate Mn (μg L $^{-1}$); (d) AS2 concentrations of dissolved and particulate Zn (μg L $^{-1}$).

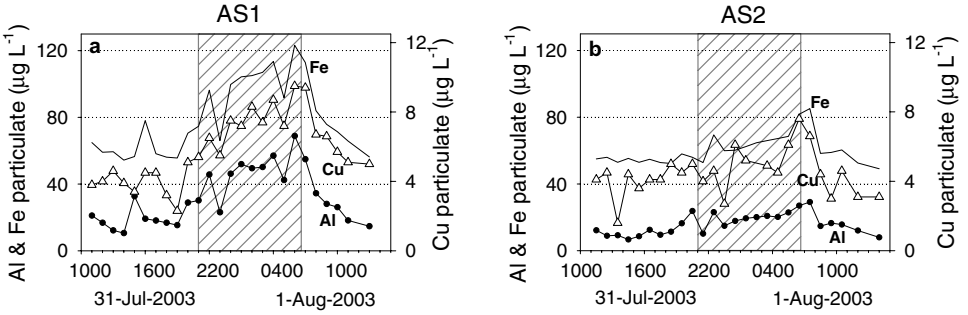

Fig. 5. Particulate concentrations of Al, Fe and Cu (μg L $^{-1}$) at AS1 (a) and AS2 (b).

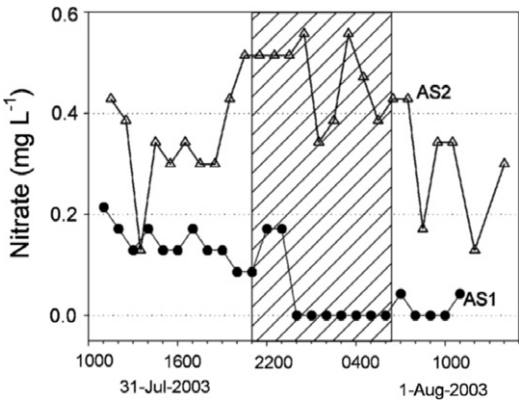

Fig. 6. Nitrate concentrations at AS1 and AS2 (mg NO_3 L $^{-1}$).

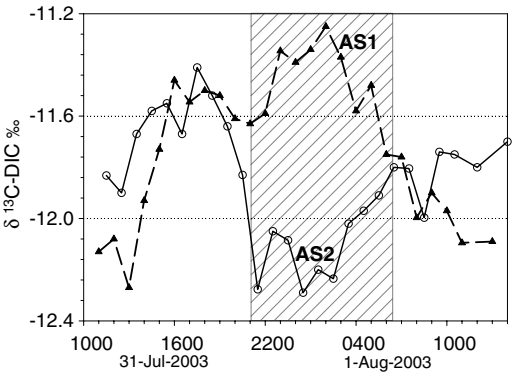

Fig. 7. The stable isotope concentration of dissolved inorganic C (δ^{13}C-DIC, ‰, VPDB) at AS1 and AS2 during the diel sampling period.

values continued to increase during the night at AS1, but decreased sharply at AS2. The differences in isotopic behavior of DIC at the two sites are believed to be linked to differences in nutrient balance and biological productivity, and are discussed in more detail below.

3.5. Chemical gradients

The ability to examine gradients in chemical and physical parameters across the study reach is an important advantage of using two simultaneous diel sampling sites. Between site changes (Δ) in pH, TA (μmol kg ^{1}), DIC (μmol kg ^{1}), δ^{13}C-DIC, DO (μmol L ^{1}) and pCO_2 (μatm) were adjusted for the 2.5-h transit time, and are shown in Fig. 8. The DIC concentration of each sample was calculated using PhreeqcI (Parkhurst and Appelo, 1999) from the appropriate hourly solution data, alkalinity, temperature and pH. The change in pCO_2 was positive between sites during the entire 24-h sampling (Fig. 8c), whereas the change in total alkalinity (Fig. 8a) increased gradually overnight and did not reach a maximum until 08:30 h.

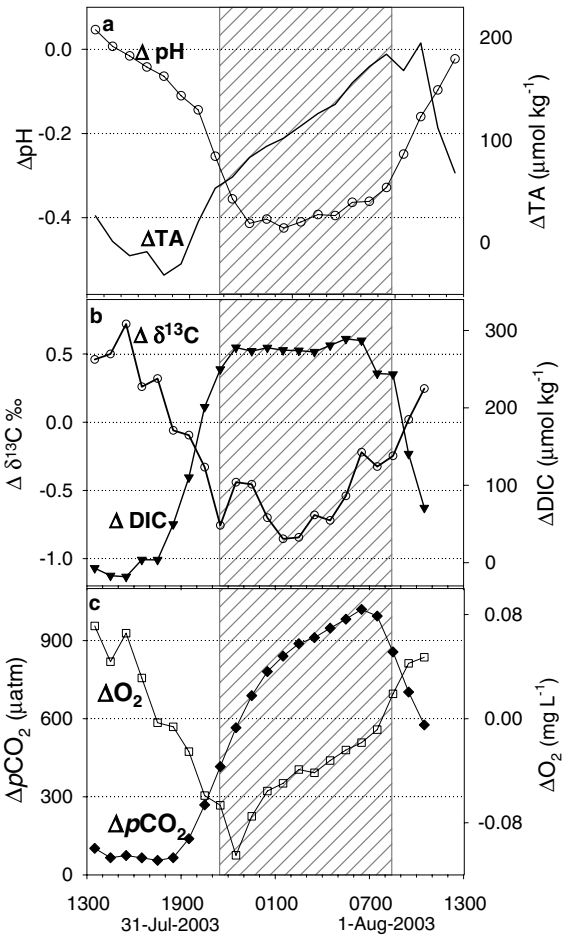

Fig. 8. Changes in chemical parameters during the 2.5 h transit between AS1 and AS2. (a) Change in pH, total alkalinity (TA, μmol kg ^{1}); (b) changes in DIC (μmol kg ^{1}) and δ^{13}C-DIC (‰); (c) changes in dissolved O_2 (μmol L ^{1}), and pCO_2 (μatm).

4. Discussion

4.1. Between site biogeochemistry

One important outcome of using the two-site sampling method is to be able to investigate the processes controlling the changes in stream chemistry. River pH is a "master variable" that is influenced by biological processes (respiration, photosynthesis), physical processes (gas and heat exchange) as well as mineral dissolution and precipitation. The ΔpH between sites is negatively correlated with the ΔpCO_2 ($R^2 = 0.86$, $p < 0.0001$) which emphasizes that pH control is being largely influenced by changes in CO_2 concentration. Additionally, $\Delta\delta^{13}$C-DIC between sites is negatively correlated with ΔpCO_2 ($R^2 = 0.77$, $p < 0.0001$). As indicated in Section 1, the control of pCO_2 through photosynthesis and respiration will have a significant influence on δ^{13}C-DIC. This is reinforced by the fact that ΔpCO_2 is positively correlated with ΔDIC ($R^2 = 0.91$, $p < 0.0001$) indicating that processes controlling the CO_2 concentration have a significant effect on the concentration of DIC. The ΔDIC reached a night-time steady state at 22:30 h (Fig. 8b) suggesting that the rate of contribution from respiration was approximately matched by the rate of CO_2 degassing.

The increase in flow between AS1 and AS2 was approximately 15% (Section 2). Consequently, 85% of the water reaching AS2 was water that was sampled at AS1 about 2.5 h earlier with the difference being tributary and groundwater influx. This is consistent with an interpretation that the major factors controlling river chemistry are in stream biological processes (photosynthesis and respiration) and physical processes (gas and heat exchange) since the majority of water flowing between sites is water that started at the upstream location.

4.2. Mechanisms controlling Mn and Zn diel concentrations

Manganese is known to undergo a photoreduction cycle in seawater (Sunda et al., 1983; Sunda

and Huntsman, 1994) and recent studies have shown a similar photoreductive cycle in streams, coupled with microbial catalysis (Scott et al., 2002; Haack and Warren, 2003). Photoreduction has been shown to increase the concentration of dissolved Fe during the day in acidic streams receiving acid rock drainage (McKnight et al., 1988; Gammons et al., 2005a; Parker et al., 2006). The diel concentration cycles observed in this and other studies in alkaline streams (Brick and Moore, 1996; Nimick et al., 2003, 2005; Jones et al., 2004) show an inverse pattern to that expected if photoreduction was the dominant process. While photoreduction may be a component of these systems, other studies have shown that photosynthetically mediated Mn(II) oxidation can lead to a net removal of dissolved Mn(II) during the day (Scott et al., 2002). Consequently, photoreduction will not be considered here as having a major influence on daily changes in trace metal concentrations.

There are a number of other possible mechanisms that could explain the observed diel cycles in dissolved Mn and Zn in the study area. These include: (1) changes in the influx of dissolved metals from the hyporheic zone or shallow groundwater; (2) pH- and temperature-dependent adsorption to benthic and suspended surfaces; (3) daytime precipitation of Mn and Zn mineral phases, or as impurities incorporated into carbonate minerals; and (4) diel cycles of oxidative precipitation during the day possibly followed by reductive dissolution at night in association with biofilms and algal communities. Each of these mechanisms will be discussed in turn.

The concentration minima and maxima for dissolved Mn and Zn at AS1 and AS2 were in phase (Fig. 4). This suggests that the concentration cycles are linked to in-stream processes, and are not the result of the downstream advection of a pulse of elevated metal concentration which would have manifested itself through the 2.5 h transit time for stream water between AS1 and AS2. In addition, discharge at AS1 showed a minimum to maximum change of only about 3%, and was not well-correlated with dissolved Mn or Zn concentrations ($R^2 = 0.35$ and 0.51, respectively). The small increase in flow during the night at AS1 was most likely caused by the cessation of evapo-transpiration by stream side vegetation. However, the concentrations of chemically conservative species such as Na, K, Li and SO_4^{2-} (data not shown) did not change over the sampling period at AS1. Together, these observations suggest that any diel contribution of flow from hyporheic water did not have a significant impact on river chemistry.

Temperature- and pH-dependent sorption to benthic or suspended sediments has been suggested as the driving force for diel metal variability in other river systems in Montana (Brick and Moore, 1996; Nimick et al., 2003, 2005; Gammons et al., 2005a; Parker et al., 2006). It is well known that adsorption of divalent metal cations onto hydrous metal oxides is favored by an increase in pH. In addition, literature values for adsorption enthalpies reported for divalent metal cations with hydrous Fe, Al and Mn oxide surfaces are endothermic at near neutral pH (Machesky, 1990; Rhodda et al., 1996; Trivedi and Axe, 1999, 2000), indicating that adsorption is also favored by an increase in temperature. The daytime decreases in dissolved Zn and Mn concentration reported here are consistent with the daytime increases in both pH and water temperature. However, the concentrations of Mn and Zn also increased in the *particulate* fractions at night, which would not be expected from a simple sorption model. Distribution coefficients (K_d, L kg^{-1}) were calculated based on a comparison of Mn and Zn concentrations in the filtered and particulate phases. At AS1 the average values ($\log K_d$) were 5.17 ($\pm$0.15) and 6.20 ($\pm$0.23) for Mn and Zn, respectively. These K_d values are comparable to literature values, such as $\log K_{d,Mn} = 5.6$ (pH 7.4) (Davide et al., 2003) and $\log K_{d,Zn} = 5.05 \pm 0.1$ (pH 7.7–8.3) (Warren and Zimmerman, 1994). The calculated distribution coefficients showed no diel patterns (data not shown), and the lack of any such change confirms that partitioning of Mn and Zn between suspended solids and the dissolved phase was not the major factor controlling the Mn and Zn diel cycles. However, it remains a possibility that sorption was occurring onto the *benthic* substrate of the stream. Morris et al. (2005) have reported that Zn diel concentration cycles were controlled by uptake to photosynthetic biofilms in High Ore Creek, MT with subsequent transfer to Mn oxide coatings on benthic surfaces. In High Ore Creek the dissolved Zn concentrations were approximately 1 order of magnitude higher than Zn in particles and also about 1 order of magnitude higher than the concentration of dissolved Mn (Nimick et al., 2003; Morris et al., 2005). These Zn and Mn concentrations in High Ore Creek are in contrast to results presented in this study which show that dissolved Mn in the CFR was about

10-fold higher in concentration than dissolved Zn. Additionally, Zn concentration in particles was about 10-fold higher than dissolved Zn. The concentration of Zn in particles at AS1 increased in phase with the dissolved Zn and Mn concentrations in the early morning (Fig. 4). While the dissolved Zn concentration cycle in the CFR may be in part controlled by sorption to biofilms, the large daily concentration change in dissolved Mn should have a significant influence on the concentrations of other trace metals such as Zn, Cu and Fe (discussed in mechanism 4 below).

The third possible mechanism, solute precipitation or co-precipitation was addressed using the geochemical modeling program PhreeqcI. The solid Mn phase that was closest to saturation based on the modeling was rhodochrosite ($MnCO_3$). However, the saturation index (SI) for $MnCO_3$ was negative during the entire sampling period (average value 0.58). The saturation index for smithsonite ($ZnCO_3$) was even more negative, averaging 3.2 for the 24-h period. These results suggest that pure Mn- or Zn-carbonate phases should not have been precipitating from the Clark Fork River water. However, it is also possible that Zn and Mn were co-precipitating with a carbonate mineral (i.e., calcite) as pH increased from 8.2 to 8.7 during the day. The SI for calcite at both sites was positive and showed an inverse relationship to the concentration of the dissolved forms of both Zn and Mn (Fig. 9, $R^2_{\text{Mn-SI}} = 0.92$ and 0.90, $R^2_{\text{Zn-SI}} = 0.50$ and 0.90, at AS1 and AS2, respectively). Biofilm and algal surfaces have been shown to form high pH microenvironments that can promote calcite precipitation during the photosynthetic period (Hartley et al., 1996; Falkowski and Raven, 1997). Consequently, the saturation index for a particular carbonate mineral at the biofilm surfaces may be higher than that calculated for the water column. Based on published partition coefficients of Mn and Zn into $CaCO_3$ solid solutions (Lorens, 1981; Zachara et al., 1991) it is likely that Mn and Zn would have readily partitioned into any calcite formed. However, the existence of a positive SI value obtained by a computer model does not prove that calcite precipitated. It has also been demonstrated that inorganic and organic phosphates and dissolved organic matter can act as nucleation inhibitors and allow supersaturation of $CaCO_3$ without significant precipitation occurring (House and Donaldson, 1986; Inskeep and Bloom, 1986; Falkowski and Raven, 1997).

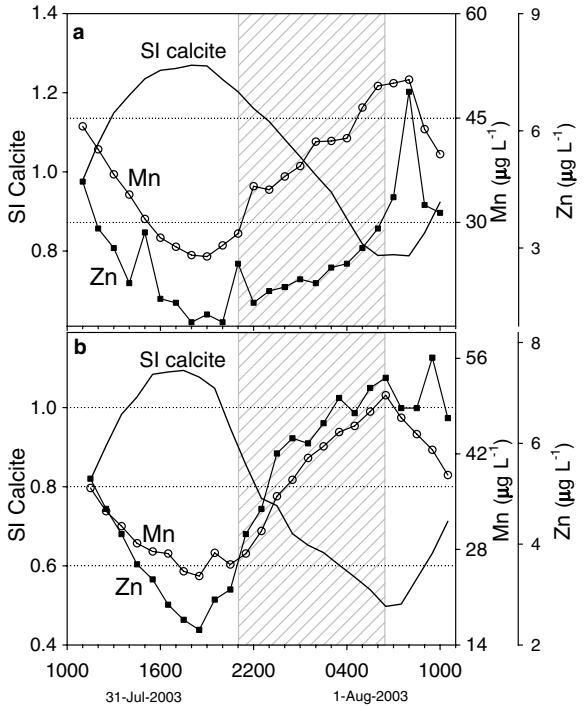

Fig. 9. (a) Saturation index (SI) for calcite at AS1 and the dissolved Mn and Zn concentrations (μg L ^{1}) and (b) SI for calcite at AS2 and the dissolved Mn and Zn concentrations (μg L ^{1}).

The authors' attempts to examine suspended solids from AS1 and AS2 collected on filters by SEM-EDX failed to identify a carbonate phase. In addition, there were no clear diel cycles in dissolved Ca or total alkalinity in the data sets, although it is probable that even a small amount of carbonate mineral precipitation would cause a substantial change in the trace metal concentration, given the very high Ca/(Mn + Zn) ratios in the water column. The hypothesis that carbonate phase dissolution or precipitation reactions influence diel cycling of Mn and Zn in the Clark Fork River could be tested further by detailed examination of mineral and biological materials coating the streambed to see if a carbonate phase is present, and to determine the approximate mole fractions of $ZnCO_3$ and $MnCO_3$ in this phase.

The authors believe the fourth proposed mechanism is most consistent with the results presented here. Previous studies have shown that photosynthetically mediated Mn(II) oxidation can lead to a net removal of dissolved Mn(II) during the day (Scott et al., 2002). Microbially catalyzed oxidation of Fe and Mn has been shown to occur in biofilms

and sediment surfaces (Ghiorse, 1984; Czekalla et al., 1985; Richardson et al., 1988; Tebo et al., 1997; Zhang et al., 2002). During photosynthesis, sharp increases in O_2 concentration and pH can occur near the surface of algal and bacterial mats which may lead to localized precipitation of hydrous ferric oxide (HFO) and hydrous manganese oxide (HMO) (Richardson et al., 1988; Olivie-Lauquet et al., 2001; Haack and Warren, 2003). The hydrous metal oxides are known to be sorbents for associated trace metals (Fuller and Harvey, 2000; Haack and Warren, 2003). Copper, Cd and Zn were shown to be highly concentrated in HMO and HFO coatings grown on ceramic beads in Silver Bow Creek (Benner et al., 1995), which is one of the headwater streams of the Clark Fork River. Zinc has a particularly high affinity for hydrous Mn oxides (Hem et al., 1984; Shope et al., 2006). At night, as photosynthesis ceases and respiration consumes O_2, the microzone conditions in the biofilms reverse, resulting in locally anoxic conditions and lower pH values. These conditions are permissive for microbially enhanced reductive dissolution of HMO and HFO, with concomitant release of Mn(II), Fe(II), Zn, and other adsorbed species back to the water column (Davison, 1993; Brick and Moore, 1996; Olivie-Lauquet et al., 2001; Scott et al., 2002).

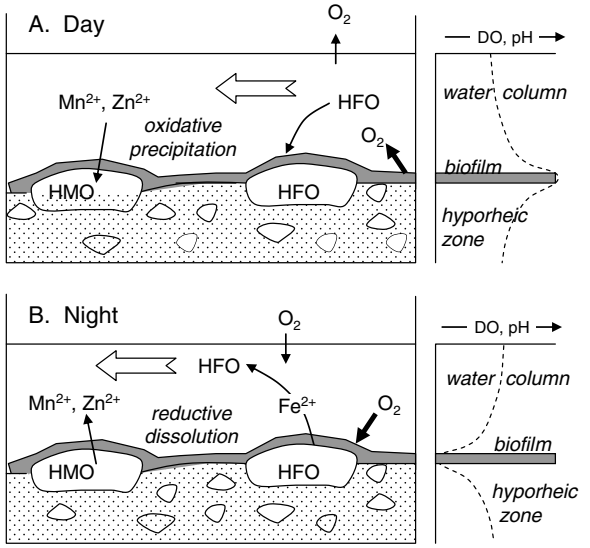

Fig. 10. Conceptual model summarizing the microbial redox hypothesis to explain diel changes in dissolved and particulate metal concentration. The shaded area represents biofilm. HMO and HFO represent gravel or boulders that are coated with hydrous oxides of Mn or Fe, respectively. The graphs on the right show approximate (not to scale) variations in pH and dissolved O_2 concentration (DO) from the water surface to the biofilm layer, and below into the shallow hyporheic groundwater. Arrows show fluxes of DO and metals into and out of the water column during the day (top) and during the night (bottom).

Fig. 10 is a conceptual model that illustrates the microbial redox cycling process outlined above. In general, the daytime period is dominated by oxidative precipitation of HFO and HMO, whereas the night is dominated by reductive dissolution. An important additional element of the model is the prediction that, once mobilized back into the aerated water column during the night-time period, dissolved Fe will re-oxidize at a much faster rate than dissolved Mn, resulting in an increase in the concentration of HFO particles at night. This hypothesis is supported by both field observations (Figs. 4 and 5) and experimental kinetic data. For example, reported values for the half-life of dissolved Mn(II) in aerated waters at pH 8 and 20 °C range from 1 to 100 days, as compared to minutes for Fe(II) at equivalent conditions (Davison, 1993). The longer half-life of Mn(II) versus Fe(II) would have allowed dissolved Mn concentration to increase during the night, whereas any dissolved Fe released to the water column would have quickly oxidized and precipitated as HFO. Other trace solutes, such as arsenate, Zn, Cu and Mn, would have adsorbed onto the freshly formed HFO particles. In the present study, the diel concentration patterns of particulate Cu and Fe (Fig. 5) were well-correlated at AS1 ($R^2 = 0.88$), although less so at AS2 ($R^2 = 0.54$). Additionally, at AS2 there was no discernable pattern in the Mn and Zn particulates (Fig. 4). The stream gradient at AS1 is steeper than at AS2 and consequently the average flow-weighted velocity at AS1 was $0.20\ m\ s^{-1}$ while at AS2 it was $0.13\ m\ s^{-1}$. It is possible that the lower velocity at AS2 allowed particles to settle to the stream bed more readily at AS2 than at AS1 such that at night an increase in particles was not observed at the downstream site.

To investigate the possibility that diel changes in O_2 concentration in the river are controlled by the net productivity of the benthic communities, Eq. (1) was used to determine if the estimated O_2 flux (F) across the sediment surface is consistent with the DO flux in the water column:

$$F = H\frac{dC}{dt} = \frac{D}{z}\Delta C \qquad (1)$$

It is assumed that the O_2 concentration approaches zero below ~2 mm within the benthic sediments (Haack and Warren, 2003) and that the O_2 gradient

across the boundary layer and in the water column is largely mediated by daytime net productivity and night-time respiration. The average river depth (H) was 17.1 and 22.3 cm at AS1 and AS2, respectively. The O_2 diffusion coefficient in water (D) used was 2.0×10^{-5} cm^2 s^{-1} (20 C; Bird et al., 1960). The biofilm layer thickness used was 0.1 cm (z) and the change in O_2 concentration across this boundary layer [ΔC, $C_{(sed)}$ $C_{(water\ column)}$] was assumed to be +300 and 50 μmol L^{-1} at 15:00 and 04:00 h, respectively (Richardson et al., 1988; Haack and Warren, 2003). The benthic flux values calculated by this method are approximations of the movement of molecular O_2 across the benthic boundary layer. A positive flux value corresponds to an excess of O_2 in the surface layer resulting in a diffusion of O_2 to the water column. A negative value means that the O_2 concentration in the sediment layer approaches zero with respect to the water. Table 1 compares the calculated O_2 benthic flux (μmol cm^{-2} h^{-1}) versus the hourly measured O_2 flux (ΔO_2) in the water column. The observed water column flux values are in relatively good agreement with the calculated benthic values. This suggests that at night, near zero O_2 concentrations existed in the bottom boundary layer.

4.3. Nutrient and carbon isotope cycling

The differences in the diel cycles of dissolved NO_3^- between AS1 and AS2 are most likely a result of nutrient inputs from irrigation return flows between the two sites which locally changed the biological productivity of the river. As discussed above (Section 3.3 and Fig. 6), dissolved NO_3^- concentrations were higher at AS2 versus AS1, and showed a nightly increase in concentration at AS2 as opposed to a nightly *decrease* at AS1. The optimal molar ratio of NO_3^- to PO_4 for algal growth is predicted to be 16:1 (Redfield et al., 1963). The downstream site was above the 16:1 ratio for most of the 24-h period while the upstream site was below this level (Fig. 11). This indicates that the AS1 site was most likely N-limited and consequently functioning at a lower productivity level. The total 24-h changes in pH, dissolved O_2, and pCO_2 were greater at AS2 than AS1 (Fig. 2), which is also consistent with a greater rate of biological activity at the downstream station.

As was the case for NO_3^-, the diel behavior of stable C isotopes was different at the two monitoring stations (Fig. 7). Both sites showed an increase in δ^{13}C-DIC starting at 13:00 h with a maximum at 17:00 h. This was followed by a decrease in δ^{13}C-DIC in the evening, which was much more apparent and long-lived at AS2 as opposed to AS1. The overall pattern is similar to that recently observed in a diel study of the isotopic composition of DIC and DO in the Big Hole River (Parker et al., 2005), a highly productive stream located 50 km south of Deer Lodge, MT. Daytime increases in δ^{13}C-DIC were linked to consumption of isotopically light CO_2 by photosynthesizing plants and algae, which enriched the remaining water column in ^{13}C. Nightly decreases in δ^{13}C-DIC were explained by the return of isotopically light biogenic CO_2 to the water column by respiration (Parker et al., 2005). The diel pattern in δ^{13}C-DIC observed in the Big Hole River is more similar to the pattern displayed at AS2 in the present study. The most likely explanation for the difference in behavior of δ^{13}C-DIC at AS1 and AS2 is the increased rates of primary productivity and respiration at the downstream station, which were most likely driven by the aforementioned inputs of NO_3^- from irrigation return flow water.

Table 1
A comparison of the O_2 flux (μmol cm^{-2} h^{-1}) calculated for the benthic surface layer and the measured flux in the river water column

Flux in O_2 (μmol cm^{-2} h^{-1})	15:00 h		04:00 h	
	Benthic calculated	River measured	Benthic calculated	River measured
AS1	0.43	0.56	0.072	0.10
AS2	0.43	0.48	0.072	0.024

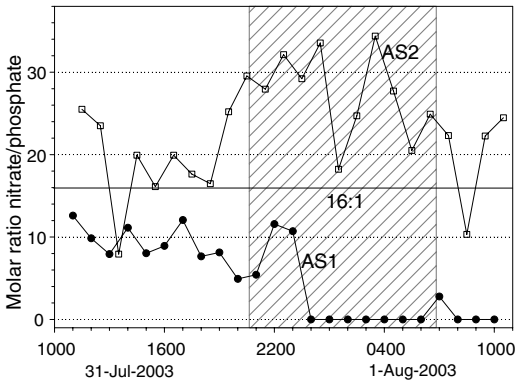

Fig. 11. Molar NO_3 to PO_4 ratios for both AS1 and AS2. The 16:1 ratio line as predicted by the Redfield equation is shown.

The above observations underscore the complexity of productive rivers such as the Clark Fork on a reach by reach scale. These results have implications for nutrient and trace metal monitoring in streams and rivers. This study has shown that very different results may be obtained depending on the time of day, and also depending on the physical location of the sampling station with respect to irrigation return waters. Recent research (e.g. Jones and Mulholland, 2000; Woessner, 2000; Poole et al., 2004) has shown that the morphology of naturally braided or meandering gravel-bed streams is conducive to exchange of shallow groundwater and surface water. Return of shallow groundwater to the main stem sets up local environments with a chemistry and/or temperature that can be quite distinct from the main stem flow. Such groundwater–surface water exchange processes are likely occurring along the upper Clark Fork River, and could well be a contributing factor to explain the complex behavior in the observed cycles of metals, nutrients, and environmental isotopes.

5. Conclusions

This study has documented diel concentration cycles for dissolved Mn and Zn and for particulate forms of Mn, Zn, Fe, Al and Cu, similar to those first reported at a nearby site on the Clark Fork River by Brick and Moore (1996). This demonstrates that the diel metal cycles are reproducible and possibly ubiquitous components of the river system. A conceptual redox cycling model was developed to explain the behavior of trace metals in the study area. In this model, hydrous oxides of Mn and Fe precipitate during the day, possibly catalyzed by autotrophic biofilms. Partitioning of other trace metals (such as Zn) into the HFO, HMO and biofilm matrix cause a daytime reduction in their concentrations. During the night, the redox gradient across the biofilm surface reverses, resulting in reductive dissolution of the HFO and HMO particles. Because of the slower rate of oxidation of Mn(II) versus Fe(II) in aerated, pH-alkaline water, most of the released Mn(II) remains in the dissolved state. In contrast, the mobilized Fe(II) is quickly re-oxidized to HFO, resulting in an increase in particulate Fe at night. Although this model explains most of the field observations, it is possible that other processes, such as cyclic dissolution/precipitation of calcite or pH-, temperature- and photoperiod-dependent adsorption processes, could also have played an important role in the diel metal cycling.

Examination of diel trends in dissolved NO_3 and the stable isotopic composition of DIC (δ^{13}C-DIC) showed large differences between the upstream and downstream station. Owing to inputs of nutrients from irrigation return flows, the river at the downstream site had a higher biological productivity, leading to larger 24-h swings in pH, DO and pCO_2. At this location, dissolved NO_3 concentrations increased during the night (as was observed previously by Brick and Moore, 1996), and δ^{13}C-DIC decreased. This result is consistent with the release of NO_3 and biogenic CO_2 by community respiration. In contrast, the upstream site showed a decrease in NO_3 concentration and a much less pronounced drop in δ^{13}C-DIC during the night. The fact that such large differences in diel behavior were noted over a relatively short stream reach underscores the spatial and temporal complexity of biogeochemical processes that occur in gravel-bed rivers. These differences emphasize the need to incorporate time- and location-dependent variability in sampling activities.

Acknowledgements

We thank Johnnie Moore and Heiko Langner of the University of Montana for help with the analytical work and David Nimick for critical discussion. J. Landskron, L. Milodragovich, D. Pellicori, B. Parker, T. Martz and M. Seidel contributed to the field work and data evaluation. S. Parker and C.H.G. were funded by EPA-EPSCoR and the Montana Board of Research and Commercialization Technology. S. Parker was also funded by the Montana Tech Faculty Seed Grant program. S. Poulson was funded in part by NSF. M.D.D. and S. Parker were funded by NSF Grant EAR-0337460.

References

Baehr, M.M., DeGrandpre, M.D., 2004. *In situ* pCO_2 and O_2 measurements in a lake during turnover and stratification: observations and modeling. Limnol. Oceanogr. 49, 330–340.

Benner, S.G., Smart, E.W., Moore, J.N., 1995. Metal behavior during surface–groundwater interaction, Silver Bow Creek, Montana. Environ. Sci. Technol. 29, 1789–1795.

Bird, R.B., Stewart, W.E., Lightfoot, E.N., 1960. Transport Phenomena. John Wiley & Sons, NY.

Bourg, A.C.M., Bertin, C., 1996. Diurnal variations in the water chemistry of a river contaminated by heavy metals. Natural biological cycling and anthropic influence. Water Air Soil Pollut. 86, 101–116.

Brick, C.M., Moore, J.N., 1996. Diel variation of trace metals in the upper Clark Fork River, Montana. Environ. Sci. Technol. 30, 1953–1960.

Clark, I.D., Fritz, P., 1997. Environmental Isotopes in Hydrogeology. Lewis Publishers, NY.

Czekalla, C., Mevius, W., Hanert, H.H., 1985. Quantitative removal of iron and manganese by micro-organisms in rapid sand filters (*in situ* investigations). Water Supply 3, 111–123.

Davide, V., Pardos, M., Diserens, J., Ugazio, G., Thomas, R., Dominik, J., 2003. Characterization of bed sediments and suspension of the river Po (Italy) during normal and high flow conditions. Water Res. 37, 2847–2864.

Davison, W., 1993. Iron and manganese in lakes. Earth Sci. Rev. 34, 119–163.

DeGrandpre, M.D., Hammar, T.R., Smith, S.P., Sayles, F.L., 1995. *In situ* measurements of seawater pCO_2. Limnol. Oceanogr. 40, 969–975.

DeGrandpre, M.D., Baehr, M.M., Smith, S.P., Hammar, T.R., 1999. Calibration-free optical chemical sensors. Anal. Chem. 71, 1152–1159.

Dickson, A.G., Afghan, J.D., Anderson, G.C., 2003. Reference materials for oceanic CO_2 analysis: a method for the certification of total alkalinity. Mar. Chem. 80, 185–197.

Duff, B.C., 2001. Arsenic treatability study utilizing aeration and iron adsorption–coprecipitation at the Warm Springs Ponds. M.S. Thesis. Montana Tech, Butte, MT, USA.

Edmond, J.M., 1970. High precision determination of titration of alkalinity and total carbon dioxide content of sea water by potentiometric titration. Deep-Sea Res. 17, 737–750.

Falkowski, P.G., Raven, J.A., 1997. Aquatic Photosynthesis. Blackwell Sciences, Malden, MA, USA.

French, C.R., Carr, J.J., Dougherty, E.M., Eidson, L.A.K., Reynolds, J.C., DeGrandpre, M.D., 2002. Spectrophotometric pH measurements of freshwater. Anal. Chim. Acta 453, 13–20.

Fuller, C.C., Davis, J.A., 1989. Influence of coupling of sorption and photosynthetic processes on trace element cycles in natural waters. Nature 340, 52–54.

Fuller, C.C., Harvey, J.W., 2000. Reactive uptake of trace metals in the hyporheic zone of a mining-contaminated stream, Pinal Creek, Arizona. Environ. Sci. Technol. 34, 1150–1155.

Gammons, C.H., Nimick, D.A., Parker, S.R., Cleasby, T.E., McCleskey, C.B., 2005a. Diel behavior of Fe and other heavy metals in a mountain stream with acidic to neutral pH: Fisher Creek, Montana, USA. Geochim. Cosmochim. Acta 69, 2505–2516.

Gammons, C.H., Wood, S.A., Nimick, D.A., 2005b. Diel behavior of rare earth elements in a mountain stream with acidic to neutral pH. Geochim. Cosmochim. Acta 69, 3747–3758.

Ghiorse, W.C., 1984. Biology of iron and manganese-depositing bacteria. Annu. Rev. Microbiol. 38, 515–550.

Grant, T.M., 2006. Hydrogeochemistry of arsenic and other trace metals in lower Silver Bow Creek below Warm Springs Ponds, Montana. M.S. Thesis. Montana Tech, Butte, MT, USA.

Haack, E.A., Warren, L.A., 2003. Biofilm hydrous manganese oxyhydroxides and metal dynamics in acid rock drainage. Environ. Sci. Technol. 37, 4138–4147.

Harris, D., Porter, L.K., Paul, E.A., 1997. Continuous flow isotope ratio mass spectrometry of carbon dioxide trapped as strontium carbonate. Commun. Soil Sci. Plant Anal. 28, 747–757.

Hartley, A.M., House, W.A., Leadbeater, B.S.C., Callow, M.E., 1996. The use of microelectrodes to study precipitation of calcite upon algal biofilms. J. Colloid Interf. Sci. 183, 498–505.

Hem, J.D., Roberson, C.E., Lind, C.J., 1984. Synthesis and stability of hetaerolite, $ZnMn_2O_4$, at 25 C. Geochim. Cosmochim. Acta 51, 1539–1547.

House, W.A., Donaldson, L., 1986. Adsorption and coprecipitation of phosphate on calcite. J. Colloid Interf. Sci. 112, 309–324.

Inskeep, W.P., Bloom, P.R., 1986. Kinetics of calcite precipitation in the presence of water-soluble organic ligands. Soil Sci. Soc. Am. 50, 1167–1172.

Jones, J.B., Mulholland, P.J., 2000. Streams and Ground Waters; Aquatic Ecology Series. Academic Press, San Diego, CA, USA.

Jones, C.A., Nimick, D.A., McCleskey, B., 2004. Relative effect of temperature and pH on diel cycling of dissolved trace elements in Prickly Pear Creek, Montana. Water Air Soil Pollut. 153, 95–113.

Lorens, R.B., 1981. Sr, Cd, Mn and Co distribution coefficients in calcite as a function of calcite precipitation rate. Geochim. Cosmochim. Acta 45, 553–561.

Machesky, M., 1990. Influence of temperature on ion adsorption by hydrous metal oxides. In: Bassett, R.L., Malchoir, D.C. (Eds.), Chemical Modeling of Aqueous Systems. I: American Chemical Society Symposium Series, vol. 416, pp. 282–292.

McKnight, D.M., Kimball, B.A., Bencala, K.E., 1988. Iron photoreduction and oxidation in an acidic mountain stream. Science 240, 637–640.

Moore, J.N., Luoma, S.N., 1990. Hazardous wastes from large-scale metal extraction. Environ. Sci. Technol. 24, 1279–1285.

Morris, J.M., Nimick, D.A., Farag, A.M., Meyer, J.S., 2005. Does biofilm contribute to diel cycling in Zn in High Ore Creek, Montana? Biogeochemistry 76, 233–259.

Nagorski, S.A., Moore, J.N., McKinnon, T.E., Smith, D.B., 2003. Scale-dependent temporal variations in stream water geochemistry. Environ. Sci. Technol. 37, 859–864.

Nimick, D.A., Moore, J.N., Dalby, C.E., Savka, M.W., 1998. The fate of geothermal arsenic in the Madison and Missouri Rivers, Montana and Wyoming. Water Resour. Res. 34, 3051–3067.

Nimick, D.A., Gammons, C.H., Cleasby, T.E., Madison, J.P., Skaar, D., Brick, C.M., 2003. Diel cycles in dissolved metal concentrations in streams – occurrence and possible causes. Water Resour. Res. 39, 1247. doi:10.1029/WR001571.

Nimick, D.A., Cleasby, T.E., McClesky, R.B., 2005. Seasonality of diel cycles of dissolved trace metal concentrations in a Rocky Mountain Stream. Environ. Geol. 47, 603–614.

Nimick, D.A., McClesky, R.B., Gammons, C.H., Cleasby, T.E., Parker, S.R., 2007. Diel mercury-concentration cycles in streams affected by mining and geothermal discharge. Sci. Total Environ. 373, 344–355. doi:10.1016/j.scitotenv.2006.11.008.

NOAA, 2006. Climate monitoring and diagnostics laboratory. Carbon Cycle Greenhouse Gases. http://www.cmdl.noaa.gov/ccgg/iadv/ (accessed November 2006).

Odum, H.T., 1956. Primary production in flowing waters. Limnol. Oceanogr. 1, 102–117.

Olivie-Lauquet, G., Gruau, G., Aline, D., Riou, C., Jaffrezic, A., Henin, O., 2001. Release of trace elements in wetlands: role of seasonal variability. Water Res. 35, 943–952.

Parker, S.R., Poulson, S.R., Gammons, C.H., DeGrandpre, M.D., 2005. Biogeochemical controls on diel cycling of stable isotopes of dissolved oxygen and dissolved inorganic carbon in the Big Hole River, Montana. Environ. Sci. Technol. 39, 7134–7140.

Parker, S.R., Gammons, C.H., Jones, C.A., Nimick, D.A., 2006. Role of hydrous iron oxide formation in attenuation and diel cycling of dissolved trace metals in a stream affected by acid rock drainage. Water Air Soil Pollut. doi:10.1007/s11270-006-9297-5 (online).

Parkhurst, D.L., Appelo, C.A.J., 1999. A computer program for speciation, batch-reaction, one-dimensional transport, and inverse geochemical calculations. U.S. Geological Survey Water Resource Investigation Report 99-4259.

Pogue, T.R., Anderson, C.W., 1994. Processes controlling dissolved oxygen and pH in the Upper Willamette River Basin. U.S. Geological Survey Water Resource Investigation Report 95-4205.

Poole, G.C., Stanford, J.A., Running, S.W., Frissell, C.A., Woessner, W.W., Ellis, B.K., 2004. A patch hierarchy approach to modeling surface and subsurface hydrology in complex flood-plain environments. Earth Surf. Process. Land. 29, 1259–1274.

Rantz, S.E., 1982. Measurement and computation of streamflow: volume 2, computation of discharge. U.S. Geological Survery Water-Supply Paper 2175, pp. 285–631.

Redfield, A.C., Ketchum, B.H., Richards, F.A., 1963. In: Hill, M.N. (Ed.), The Sea, vol. 2. Wiley, New York (Chapter 2).

Rhodda, D.P., Johnson, B.B., Wells, J.D., 1996. Modeling of the effect of temperature on adsorption of lead(II) and zinc(II) onto goethite at constant pH. J. Colloid Interf. Sci. 184, 365–377.

Richardson, L.L., Aguilar, C., Nealson, K.H., 1988. Manganese oxidation in pH and O_2 microenvironments produced by phytoplankton. Limnol. Oceanogr. 33, 352–363.

Scott, D.T., McKnight, D.M., Voelker, B.M., Hrncir, D.C., 2002. Redox processes controlling manganese fate and transport in a mountain stream. Environ. Sci. Technol. 36, 453–459.

Shope, C.L., Xie, Y., Gammons, C.H., 2006. The influence of hydrous Mn–Zn oxides on diel cycling of Zn in an alkaline stream draining abandoned mine lands. Appl. Geochem. 21, 476–491.

Silva, S.R., Doctor, D.H., Kendall, C., Chang, C.C., Fleenor, W.E., 2004. Assessing spatial and temporal variability in aquatic photosynthesis and respiration with oxygen and carbon stable isotopes. EOS Trans., AGU, 85(47) (Abstract B21C-0904).

Spiro, B., Pentecost, A., 1991. One day in the life of a stream – a diurnal inorganic carbon mass balance for a travertine-depositing stream (Waterfall Beck, Yorkshire). Geomicrobiol. J. 9, 1–11.

Sunda, W.G., Huntsman, S.A., 1994. Photoreduction of manganese oxides. Mar. Chem. 46, 133–152.

Sunda, W.G., Huntsman, S.A., Harvey, G.R., 1983. Photoreduction of manganese oxides in seawater and its geochemical and biological implications. Nature 301, 234–236.

Tebo, B.M., Ghiorse, W.C., Waasbergen, L.G., Siering, P.L., Caspi, R., 1997. Geomicrobiology: interactions between microbes and minerals. In: Banfield, J.F., Nealson, K.H. (Eds.), Min. Soc. Am., Rev. Mineral. 35, pp. 225–266.

Tobias, C.R., Bohlke, J., 2004. Diel variation of oxygen and inorganic carbon in a high productivity, high alkalinity stream: biological and geochemical controls. EOS Trans., AGU, 85(47) (Abstract H51G-07).

To, T.B., Nordstrom, D.K., Cunningham, K.M., Ball, J.W., McCleskey, R.B., 1999. New method for the direct determination of dissolved Fe(3+) concentration in acid mine waters. Environ. Sci. Technol. 33, 807–813.

Trivedi, P., Axe, L., 1999. A comparison of strontium sorption to hydrous aluminum, iron and manganese oxides. J. Colloid Interf. Sci. 218, 554–563.

Trivedi, P., Axe, L., 2000. Modeling of Cd and Zn sorption to hydrous metal oxides. Environ. Sci. Technol. 34, 2215–2223.

Usdowski, E., Hoefs, J., Menschel, G., 1979. Relationship between ^{13}C and ^{18}O fractionation and changes in major element composition in a recent calcite-depositing spring – a model of chemical variations with inorganic $CaCO_3$ precipitation. Earth Planet. Sci. Lett. 42, 267–276.

Warren, L.A., Zimmerman, A.P., 1994. The influence of temperature and NaCl on Cd, Cu and Zn partitioning among suspended particulate and dissolved phases in an urban river. Water Res. 28, 1921–1931.

Watson, V., 1989. Maximum levels of attached algae in the Clark Fork River. Proc. Mont. Acad. Sci. 49, 27–35.

Woessner, W.W., 2000. Stream and fluvial plain ground water interactions: rescaling the hydrogeologic thought. Ground Water 38, 423–429.

Wood, S.A., Gammons, C.H., Parker, S.R., 2006. The behavior of REE in naturally and anthropogenically acidified waters. J. Alloy Compd. 418, 161–165. doi:10.1016/j.jallcom.2005.07.082.

Zachara, J.M., Cowan, C.E., Resch, C.T., 1991. Sorption of divalent metals on calcite. Geochim. Cosmochim. Acta 55, 1549–1562.

Zhang, J.-H., Lion, L.W., Nelson, Y.M., Shuler, M.L., Ghiorse, W.C., 2002. Kinetics of Mn(II) oxidation by *Leptothrix discophora* SS1. Geochim. Cosmochim. Acta 65, 773–781.